Advance Researches in Civil Engineering
ISSN: 2645-7229, Vol.6, No.4, pages:31-48

Numerical Investigation of Bracing Configuration Efficiency on the Seismic Performance of High-Rise Buildings Considering Soil–Structure Interaction

***Yasir Mahdi Mahmood Al-Attar* [1], *Mohsen Seyedi* [2*]**

[*1,2] *Department of Civil Engineering, School of Engineering and Architecture, Altınbaş University, 34218 Istanbul, Turkey*

[*] *(Email: mohsen.seyedi@altinbas.edu.tr)*

(Date of received: 02/08/2024, Date of accepted: 10/11/2024)

ABSTRACT

Soil–structure interaction (SSI) alters stiffness, damping, and load paths in braced high-rise frames, but the comparative efficiency of bracing layouts under SSI remains insufficiently quantified. This study numerically evaluates a 15-story reinforced-concrete frame on clay soil using Hardening soil with small-strain stiffness soil model (HSsmall)using PLAXIS 2D, testing five steel bracing configurations—X, K, V, inverted-V, and single diagonal—subjected to three recorded earthquakes (Northridge, Imperial Valley, Kocaeli). Response metrics include interstory drift ratio (IDR), roof displacement relative to the moving base, raft rotation, and settlement. The bracing schemes and the small-strain soil formulation are detailed to ensure like-for-like comparison under SSI. Across free-vibration checks, SSI lengthened the fundamental period relative to a rigid base, confirming the role of foundation compliance. Under Northridge and Imperial Valley, bracing reduced peak IDR by ~44–48% and ~46% (from ~1.01% and 0.80% to 0.43–0.56%), with K and X consistently top performers and the diagonal layout least effective. For Kocaeli, drift gains were smaller (31–37%), reflecting longer-period content and narrowing performance gaps. Roof-drift reductions were modest overall, whereas bracing frequently increased foundation rotation (with record dependence), revealing a drift–foundation-demand trade-off under SSI. These results indicate that configuration choice under SSI is motion-dependent; K/X provide robust drift control, but designers should verify raft serviceability where stiffening could elevate rocking and settlement demands.

Keywords:

Soil-structure interaction, Steel bracing, Seismic analysis, Interstory drift ratio, Foundation rotation.

1. Introduction

Braced frames are a common lateral system for high-rise buildings [1], where columns act as chords and diagonal members carry horizontal shear primarily in axial tension–compression essentially forming a vertical truss. Adding bracing increases lateral stiffness and shifts natural frequencies [2], but when the foundation interacts with deformable soils the global response is additionally governed by soil–structure interaction (SSI)[3]. SSI alters the effective stiffness of the soil–foundation–structure system, lengthens the fundamental period [4],[5], and modifies energy dissipation mechanisms; therefore, evaluating bracing efficiency without SSI can misrepresent true seismic demands [5],[6].

Prior studies consistently show that bracing reduces interstory drift and roof displacement and can raise base shear carried by the braces themselves [8], [9], [10], with layouts such as X, V, inverted-V, zipper, and K often outperforming bare frames [11], [12]. However, much of this evidence is established for fixed-base models or without an explicit SSI treatment, leaving open how the ranking of layouts changes once foundation compliance and soil nonlinearity are included. Moreover, SSI can increase periods and amplify deformations on soft soils, reinforcing the need for layout comparisons that are explicitly SSI-aware [13].

This paper addresses that gap by performing a like-for-like numerical comparison of five bracing configurations—diagonal, X, V, inverted-V, and K—on a 15-story reinforced-concrete frame modeled as a coupled soil–foundation–structure system in PLAXIS 2D [14]. The soil is represented with HSsmall to capture strain-dependent stiffness decay and hysteretic damping [15]; the foundation is a shallow raft with compliant soil–structure interfaces; and dynamic boundaries (free-field/compliant base) are used to represent the semi-infinite soil medium [16] by absorbing out going seismic waves, rather than reflecting them back into the model. Three recorded earthquakes are applied, and responses are extracted consistently across layouts. interstory drift ratio (IDR) is measured as it is a good damage indicator for buildings and it correlates directly with structural and non-structural damage because it measures story-level deformation demand [17] , for a global measure for lateral flexibility and overall dynamic response, roof displacement relative to the base is also measured[18]. Foundation rotation from raft corner verticals is recorded as direct SSI-sensitive metric that quantifies how much lateral response is accumulated by base rocking [19] , settlement of foundation is taken from the midpoint of foundation base and measured as foundations tend to settle during earthquakes and it is shown to effect IDR ratio[20].

The study's contribution is twofold: (i) a direct, configuration-by-configuration efficiency comparison that is SSI-aware rather than fixed-base, and (ii) an explicit examination of the trade-off between improved drift control and increased foundation demands (rotation and settlement) that may accompany stiffening. The results are intended to inform selection of bracing layouts for high-rise buildings on soft clays by balancing drift targets against raft serviceability and soil performance.

2. Background

2.1. Soil–Structure Interaction (SSI)

SSI is the coupled response of the soil–foundation–structure system during seismic loading [21]. Compared with an idealized fixed base, foundation compliance and soil deformability modify the system stiffness and energy dissipation, typically lengthening the fundamental period and altering the motion transmitted into the superstructure. In numerical models, realistic far-field behavior requires "open" boundaries (transmitting/viscous or infinite elements) to absorb outgoing waves and avoid artificial reflections that would otherwise amplify response. Transmitting/infinite

boundaries substantially reduce spurious wave reflections and lower maximum lateral displacements especially on loose to medium soils where SSI effects are strongest [22].
For constitutive modeling, HSsmall (Hardening Soil with small-strain stiffness) is well suited because it captures the strong decay of shear modulus with cyclic strain and introduces amplitude-dependent hysteretic damping—key ingredients for SSI realism under earthquakes. The paper explains that HSsmall was chosen precisely for these small-strain features and drained cyclic behavior, with parameters calibrated to reproduce modulus reduction [23]. It is also demonstrated that the HSsmall model predicts the settlement in acceptable accuracy with field data [24]. The paper also provides the standard HSsmall relations for secant/tangent moduli versus shear strain (including the role of threshold strain $\gamma 0.7$), and notes that small supplemental Rayleigh damping (≈5% around target frequencies) is added (figure to the inherent hysteretic damping of HSsmall which is formulated in finite element modeling based on mass and stiffness and defined by [25], [26]:

$$C = \alpha[M] + \beta[K] \quad (1)$$

Where [M] and [K] are the mass and stiffness matrix and α and β are the Rayleigh damping coefficients.

2.2. Braced Frames in Seismic Response

Braced frames enhance lateral stiffness and strength by developing axial forces in diagonals functioning as a vertical truss that limits story drifts and roof displacement relative to bare moment frames. Comparative studies compiled in our source report that common layouts (X, V, inverted-V, zipper, K) consistently reduce interstory drift and often shift seismic demand into the braces themselves; several works identify X/K as especially effective in shortening the period and lowering roof displacement, while V/inverted-V and zipper systems also deliver strong drift control. The document further notes configuration-specific behaviors under brace buckling (e.g., chevron systems inducing beam vertical forces and potential mid-span hinging) and how zipper columns/hat trusses can redistribute post-buckling forces to mitigate soft-story mechanisms.
For clarity in the present work, the five configurations are defined as: single Diagonal; X (crossed); Inverted-V (diagonals meeting at beam mid-span above); V (meeting below); and K (diagonals framing into column mid-height). These definitions match the modeling used in our numerical program and provide a consistent basis for efficiency comparisons under SSI.

3. Numerical Methodology

3.1. Prototype Building and Foundation

A 15-story, 3-bay reinforced-concrete frame was adopted from [27]. Columns and slabs were modeled with plate elements; the story height is 3 m, and each bay is 4 m. Sectional stiffness (EA, EI) followed a zoned scheme along the height to reproduce the reference prototype's stiffness distribution (Table 1).

Table 1. Building parameters

Element	EI (kN.m^2)	EA (kN)	Unit weight (kN/m/m)
1-3 column	160,730	9,030,000	24
4-7 column	109,870	7,525,000	24
8-11 column	71,940	6,020,000	24
11-15 column	44,550	4,816,000	24
Floor slab	117,187	22,500,000	24
Damping Ratio		5%	

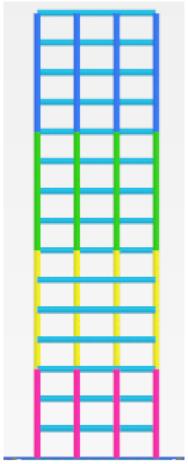
Figure 1. adopted 2D 15 story model.

The foundation is a shallow raft 15 m wide, placed at ground level with 1 m embedment. It was modeled as linear-elastic concrete (E = 30.1 GPa, G = 12.5 GPa, ν = 0.20, γ = 24 kN/m³)[27], connected to the superstructure by plate elements with pinned joints. PLAXIS interface elements were generated along the raft–soil contact to allow slip/separation. The raft is quasi-rigid relative to the soft clay (E_0≈180 MPa), ensuring period elongation, IDR, and rotation reflect soil compliance rather than raft flexibility; mesh refinement was increased at raft edges.

Table 1. Foundation parameters

Element	E (GPa)	G (GPa)	ν (–)	Unit weight (kN/m³)
Foundation raft	30.1	12.5	0.20	24

3.2. Soil Model and Domain

The soil is clay modeled with HSsmall under drained conditions to capture small-strain stiffness and hysteretic damping and to account for the stress dependency of secant shear stiffness (Gs/G0) with increasing shear strain (γ) [28]. Adopted parameters [27] are given in Table 3. Groundwater is assumed below bedrock; pore pressures were not activated in the dynamic phases.

Table 2. Soil parameters

Soil Property	Symbol	Value	Unit
Unit weight	γ	19.0	kN/m³
Poisson's ratio	ν	0.20	—
Cohesion (effective)	c′	10.0	kPa
Friction angle (effective)	φ′	27.5	degrees
Dilatancy angle	ψ',	0.0	degrees
Overconsolidation ratio	OCR	1.80	—
Coefficient of lateral earth preasure at rest	K_0	0.77	—
Threshold shear strain (Gs≈0.722·G0)	γ0.7	1.0×10^{-4}	—
Small-strain shear modulus (ref.)	$G0^{ref}$	75,000	kPa
Oedometer stiffness (ref.)	$Eoed^{ref}$	20,000	kPa
Unload–reload stiffness (ref.)	Eur^{ref}	60,000	kPa
Secant stiffness (triaxial, ref.)	$E50^{ref}$	20,000	kPa
Stress-dependency exponent	m	0.50	—
Reference pressure	pref	100	kPa

A plane-strain domain was discretized with 15-noded triangular elements as recommended by [29]-[30]. Free-field boundaries and a compliant base were used as proposed by [31] to represent the unbounded medium; interfaces were assigned at the raft–soil contact and model boundaries. Local mesh refinement was applied near the raft (coarseness factor ≈ 0.3) and relaxed toward the far field (≈ 1.0).

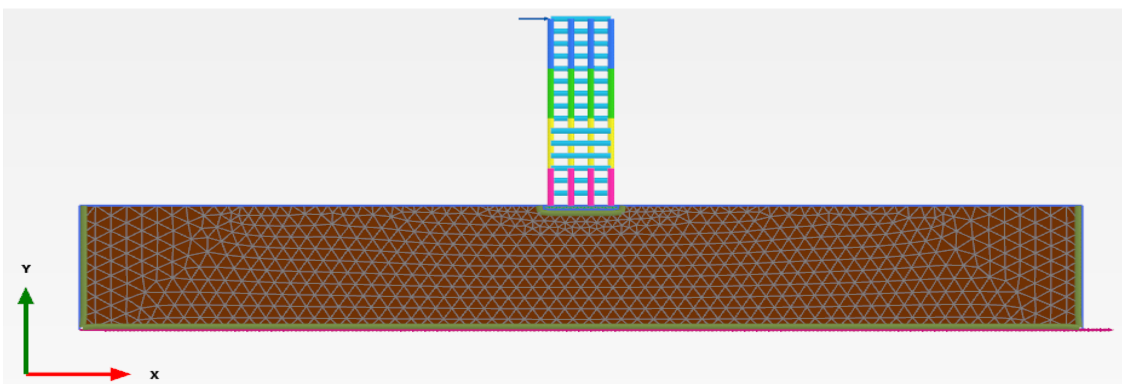

Figure 2. SSI model mesh.

3.3. Bracing Configurations and Member Modeling

All bracing layouts use a single steel section adopted from [32]: CHS 139.7×4 mm. Braces were implemented as node-to-node anchors (axial-only), with out-of-plane thickness 1.0 m. Using A = 1696 mm² and E = 210 GPa gives EA = 3.56×10^8 N (≈ 356.2×10^3 kN). Five configurations are compared: Diagonal, X, Inverted-V, V, and K; story-by-story definitions follow common practice (e.g., X braces connect opposite beam–column joints; K braces frame into columns at mid-height).

Advance Researches in Civil Engineering
ISSN: 2645-7229, Vol.6, No.4, pages:31-48

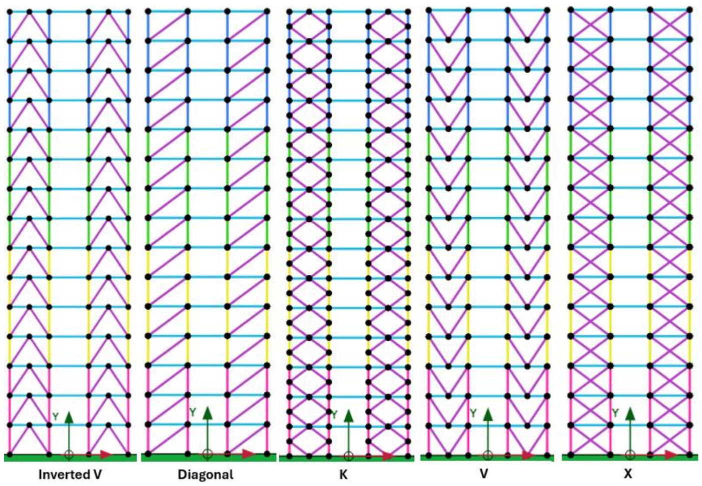

Figure 3. Bracing configurations

3.4. Ground Motions and Scaling

Three recorded horizontal components were applied at the compliant base with free-field sides, each analyzed over a 20 s window at its recorded amplitude: Northridge (1994) with PGA of 0.568 g, Imperial Valley (1979) with PGA of 0.29 g, and Kocaeli (1999) with PGA of 0.20 g.

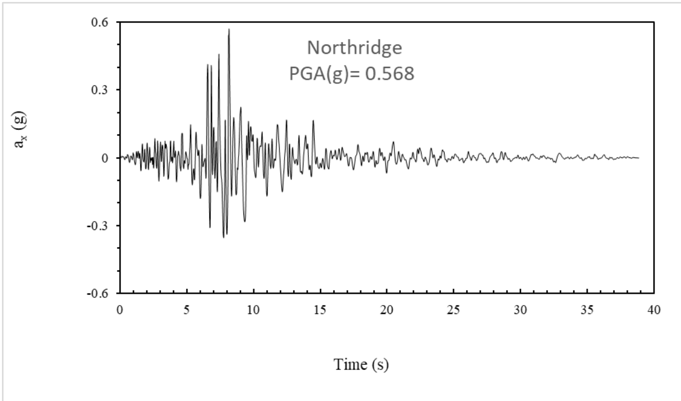

Figure 4. Northridge earthquake record.

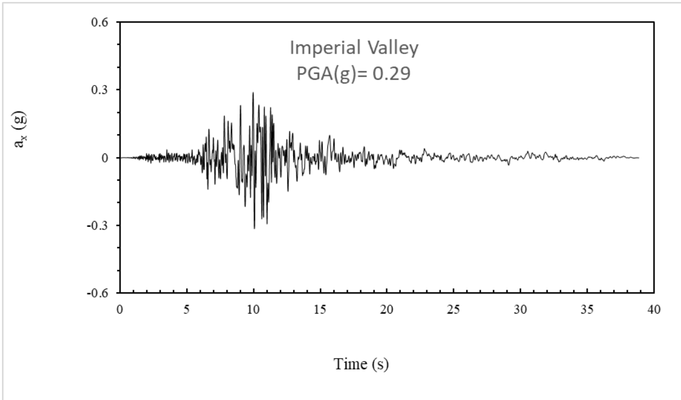

Figure 5. Imperial valley earthquake record.

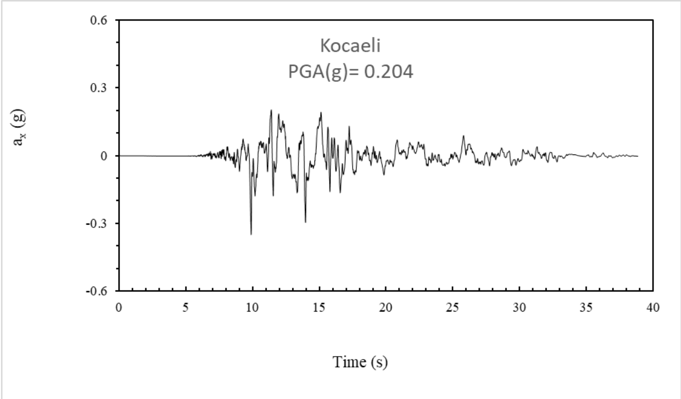

Figure 6. Kocaeli earthquake record.

3.5. Model Validation

Free-vibration tests established the mass–stiffness realism and quantified SSI-induced period by recording the lateral displacement at the top story and taking the interval between two consecutive displacement peeks: $T_1 = 2.1$ s on a rigid base versus $T_1 = 2.6$ s with SSI (HSsmall clay), consistent with foundation compliance expectations.

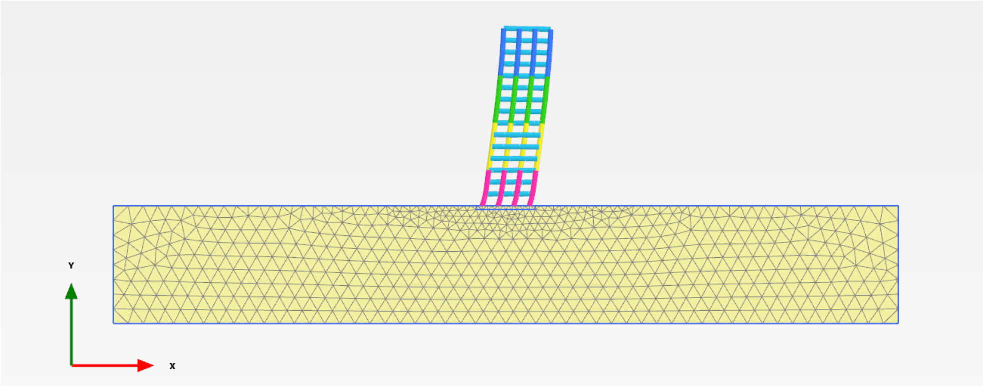

Figure 7. Deformed mesh of free vibration on rigid base.

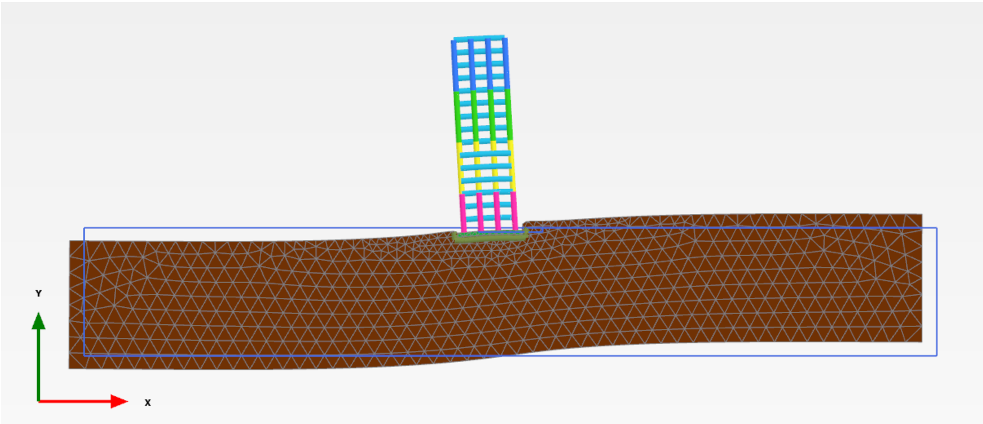

Figure 8. Deformed mesh of free vibration on flexible base.

3.6. Response Metrics and Extraction

Interstory Drift Ratio (IDR).

Story displacements were sampled at floor mid-spans per record and layout; the peak IDR over height was used for comparison.

$$IDR_i = \frac{d_{i+1} - d_i}{h_i} \tag{2}$$

Where d indicates horizontal displacement, i represent floor level and h indicates story height. Story displacements were sampled at floor mid-spans per record and layout; the peak IDR over height was used for comparison.

Roof Displacement (relative).

$$v_{roof} = v_{top} - v_{base} \tag{3}$$

removing rigid base translation and isolating lateral deformation/rocking effects.

Foundation Rotation.

$$\theta = \tan \frac{W_R - W_L}{B} \tag{4}$$

Where W_R and W_L is the right and left vertical displacement in displacement at the bottom foundation corner.

Foundation Settlement.

Vertical displacement time history at the raft center of mass; peak/permanent values extracted directly.

4. Results

4.1. Free-Vibration Findings

Free-vibration analyses revealed clear SSI-induced period elongation. The fundamental period increased from ≈2.1 s on a rigid base to ≈2.6 s when the flexible soil–foundation system was modeled, confirming that foundation compliance softens the global system prior to seismic excitation and supporting the model validation step.

4.2. Interstory Drift Ratio (IDR)

Across all ground motions, adding bracing consistently reduced peak drift demands relative to the unbraced frame. Under Northridge, peak IDR dropped by about 44–48%; under Imperial Valley by 42–47%; and under Kocaeli by 31–37%. The ranking was stable: K- and X-bracing delivered the largest reductions, while a single diagonal was least effective. These trends indicate that, even with SSI present, brace layout governs drift control effectiveness.

Advance Researches in Civil Engineering
ISSN: 2645-7229, Vol.6, No.4, pages:31-48

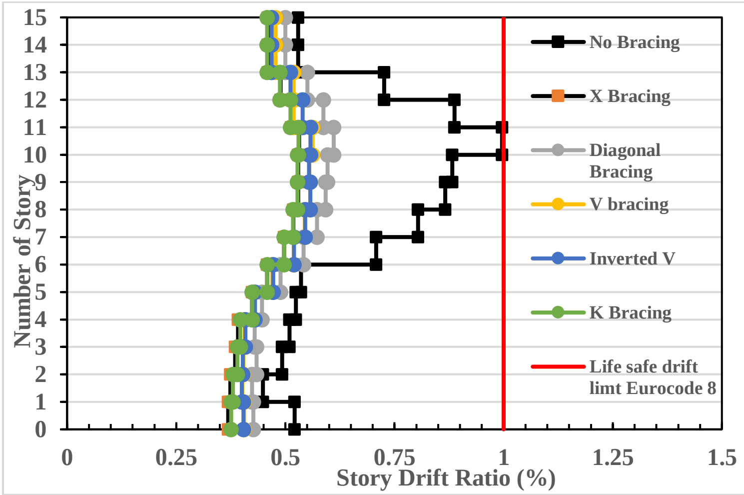

Figure 9. IDR results of Northridge record.

Under the Northridge record (Figure 9), the unbraced frame shows the largest drift, peaking in the mid to upper stories. All steel bracing sit comfortably behind the adopted drift limit according to the Eurocode 8 [33] with K and X bracing performing the best and Diagonal bracing being the least effective. A similar trend can be seen in the Imperial valley (Figure 10) record though being a relatively weaker earthquake, it still shows the improvement in performance with the added bracing. Drift increases substantially relative to the previous records with the Kocaeli earthquake (Figure 11), as usual the unbraced frame performs the worst, reaching drifts to 1.25% at the base and exceeds the adopted life safe limit. K bracing performs the best as well in this record followed by the X bracing as a close second and similarly to other records, diagonal bracing performs the least**.**

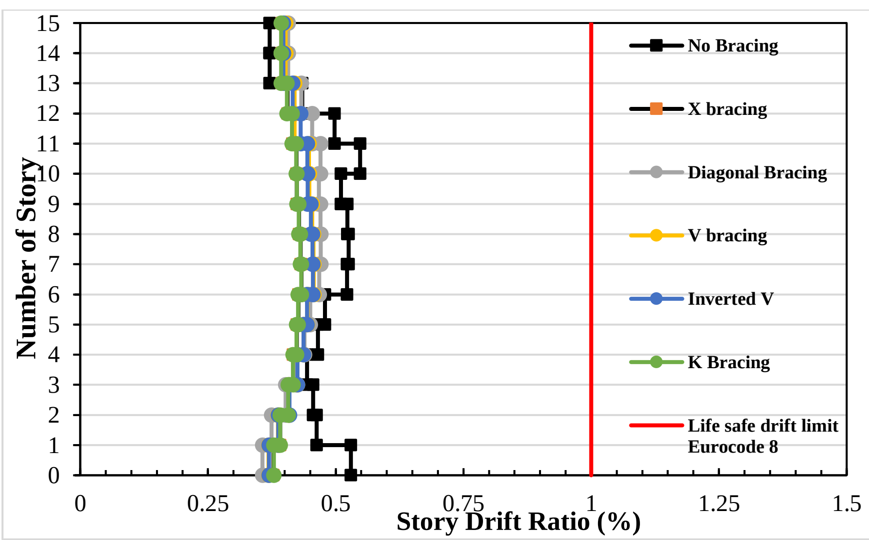

Figure 10. IDR results of Imperial Valley Record

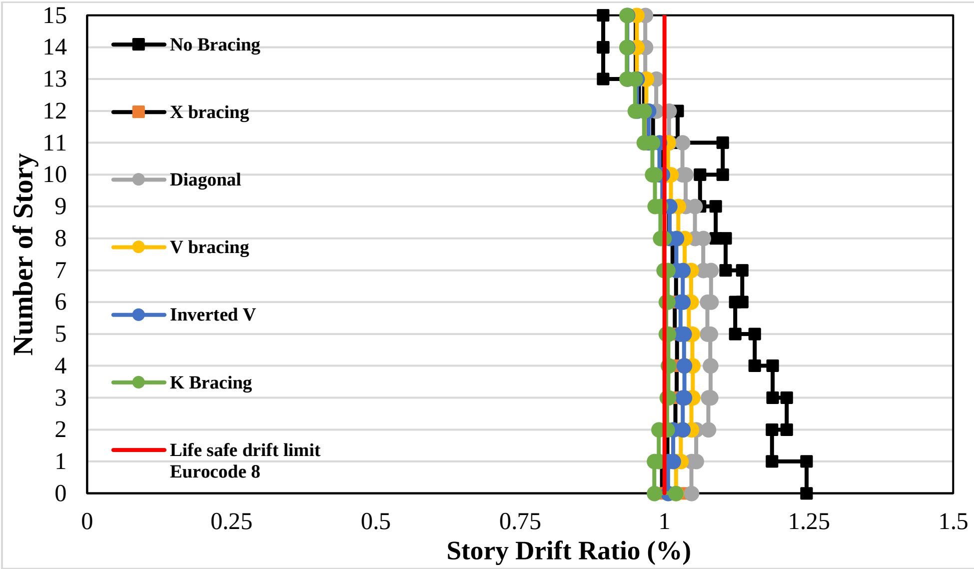

Figure 11. IDR results of Kocaeli record

4.3. Roof Displacement (Relative)

Improvements at roof level were modest compared with story drifts. Typical reductions in peak relative roof displacement were on the order of 2–11%, reflecting the combined influence of brace stiffening and base flexibility under SSI.

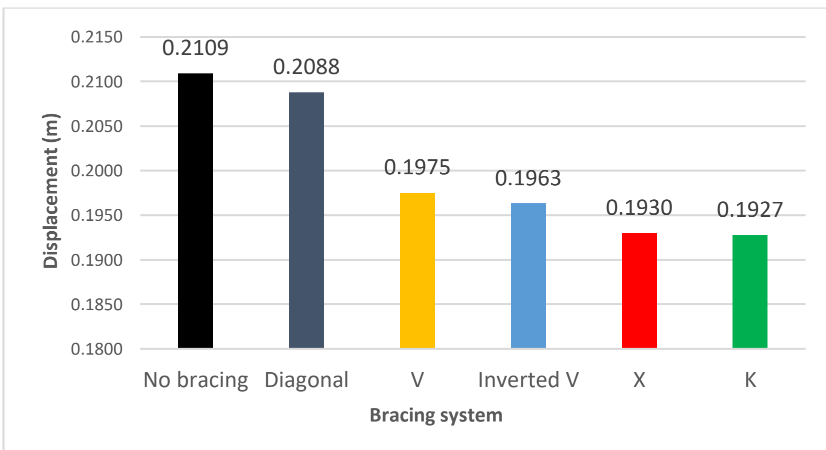

Figure 12. Top story displacement results for Northridge record.

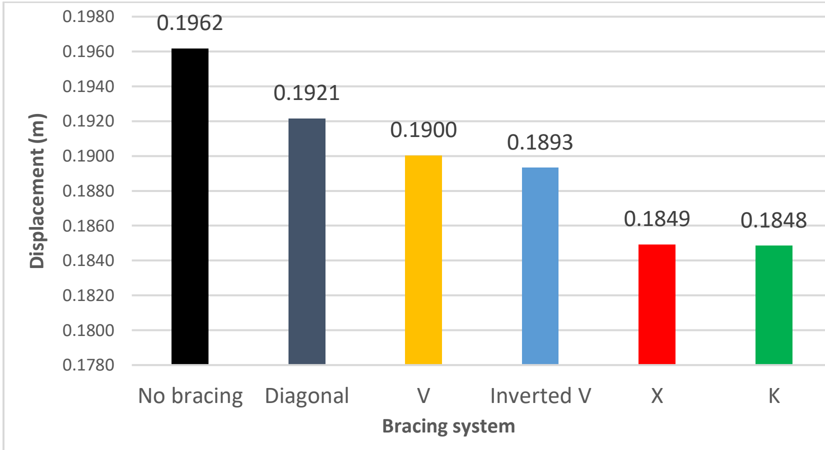

Figure 13. Top story displacement results for Imperial Valley record

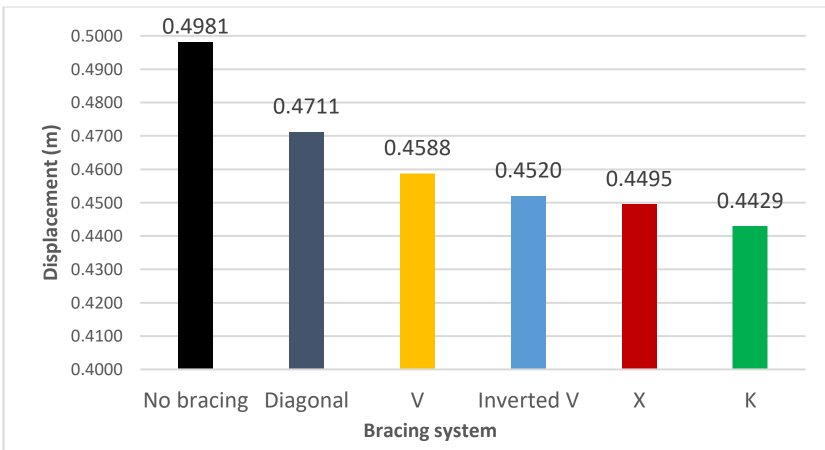

Figure 14. Top story displacement results for Kocaeli record.

4.4. Foundation Rotation

Reductions in superstructure drift did not universally translate to lower foundation rocking. For the Northridge and Imperial Valley records, bracing tended to increase raft rotation relative to the unbraced case; under Kocaeli, rotation responses for braced and unbraced schemes were broadly similar. This highlights a drift–rotation trade-off introduced by stiffening the frame atop a compliant base.

Advance Researches in Civil Engineering
ISSN: 2645-7229, Vol.6, No.4, pages:31-48

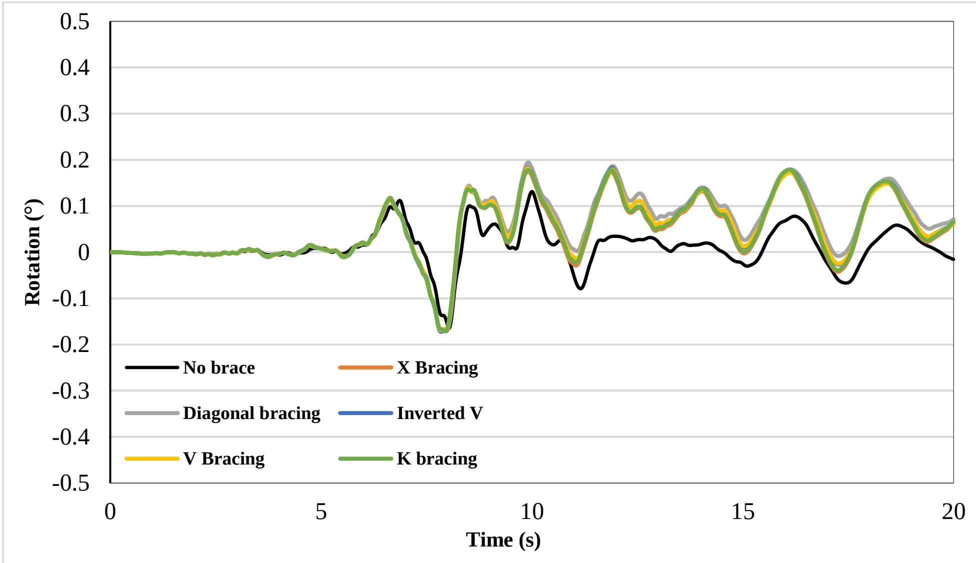

Figure 15. Foundation rotation results for Northridge record

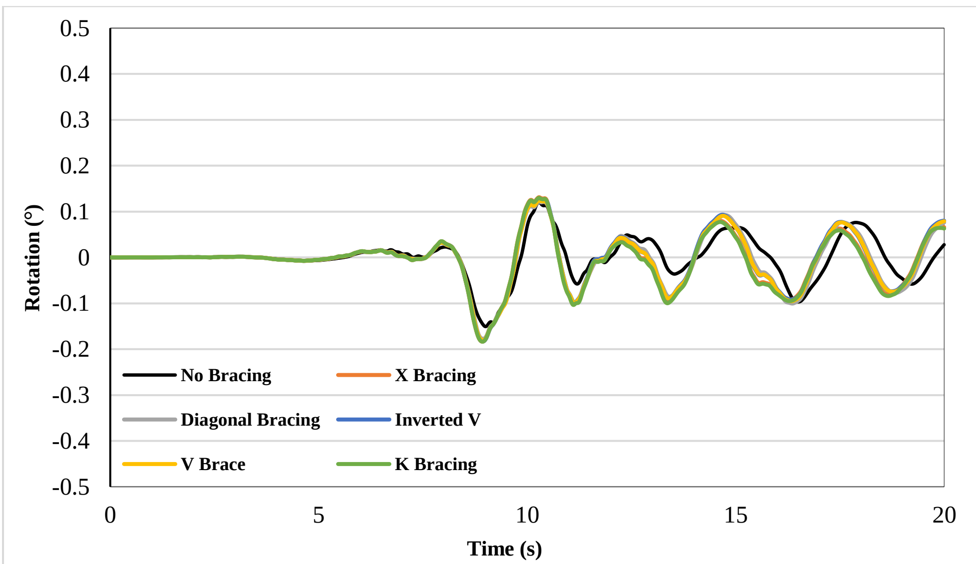

Figure 16. Foundation rotation results for Imperial valley record.

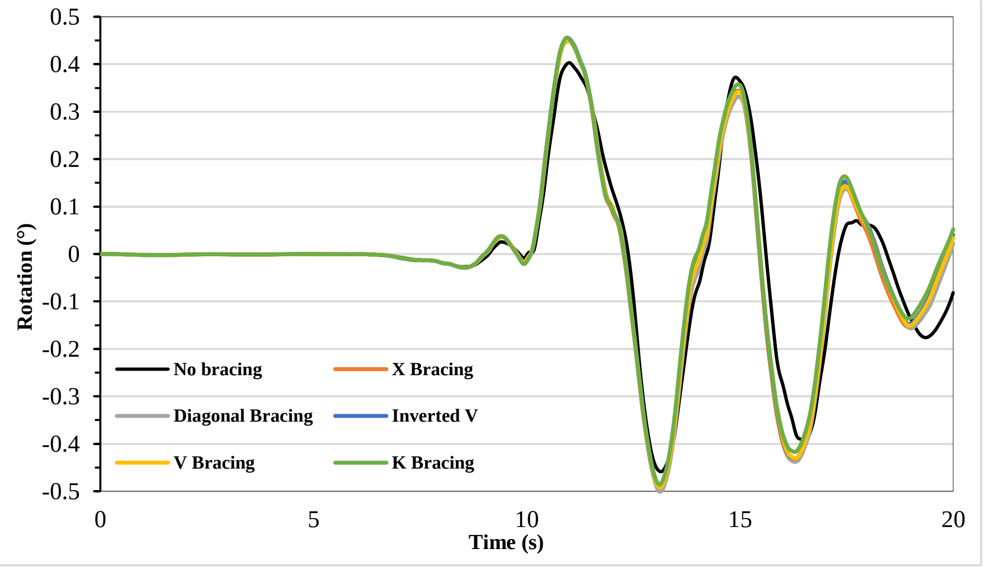

Figure 17. Foundation rotation results for Kocaeli record.

4.5. Settlement

Settlement responses were record dependent. Under Northridge, braced configurations exhibited greater permanent settlement than the unbraced frame. In contrast, under Kocaeli the braced schemes moderated both oscillatory settlement response and the accumulated (permanent) settlement compared with the unbraced model. Overall, while bracing is effective for controlling drift under SSI, configuration selection should balance superstructure benefits against potential increases in rotation and settlement at the foundation level.

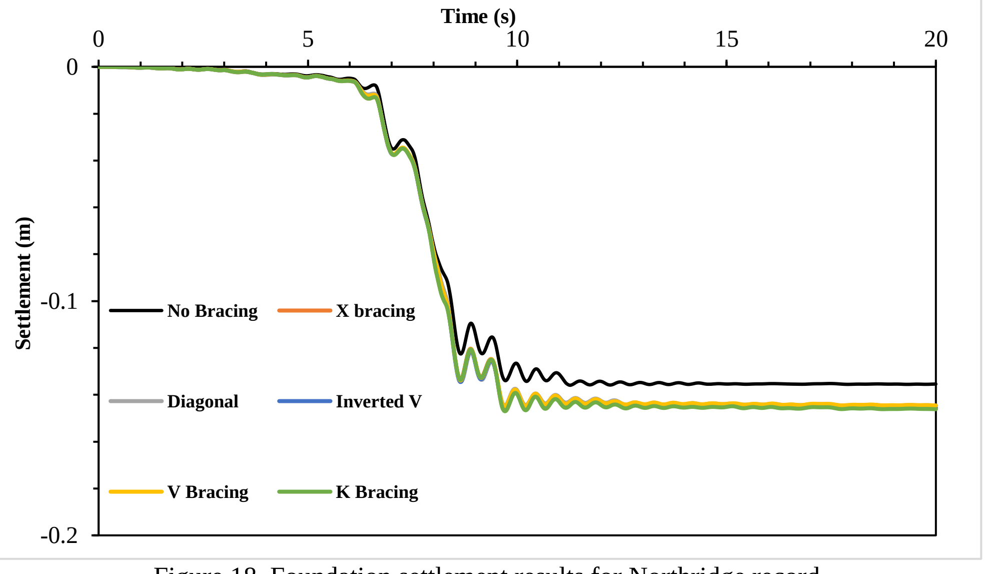

Figure 18. Foundation settlement results for Northridge record.

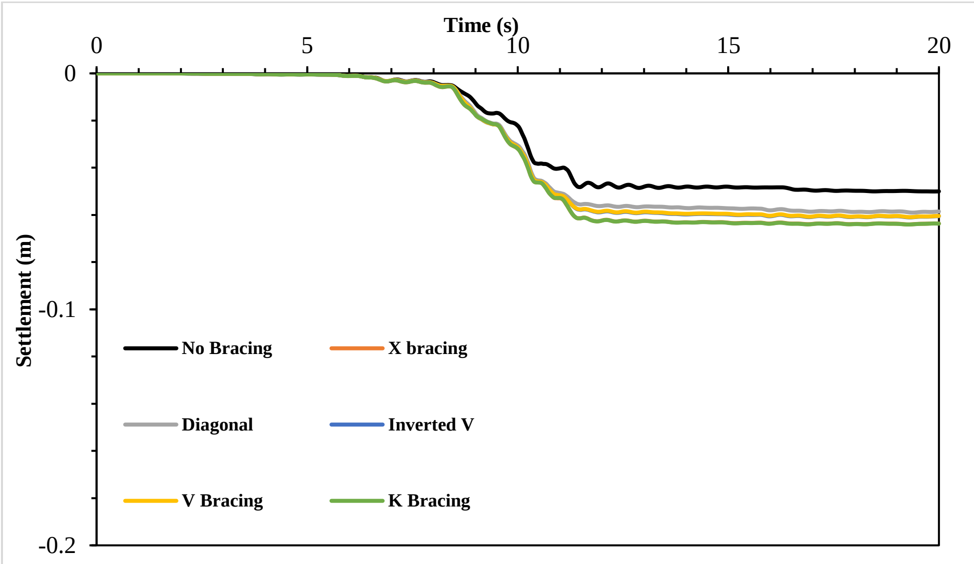

Figure 19. Foundation settlement results for Imperial valley record.

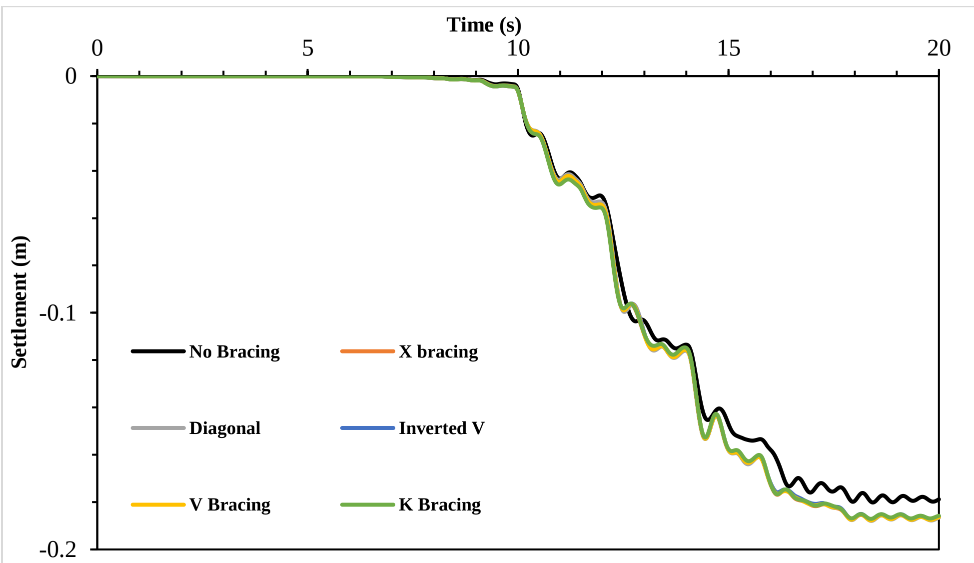

Figure 20. Foundation settlement results for Kocaeli record.

5. Discussion

The results show a clear hierarchy of bracing efficiency under SSI: K- and X-bracing provide the largest reductions in IDR across all records, followed by V and inverted-V, with single diagonal being the least effective. However, the degree of improvement depends on the motion: reductions are strongest for Northridge and Imperial Valley, while for Kocaeli, the longer-period content reduces performance gaps between the bracing layouts. While bracing effectively controls story drift, the improvements at the roof are modest, typically in the single digits. This indicates that once SSI is included, base compliance and rocking limit how much roof motion can be reduced by superstructure stiffening alone. This trend is consistent across all three records, with K providing the largest roof benefit (~7–8%) in Northridge, but overall, roof displacements remain small compared to the IDR reductions. A key finding is the drift–foundation trade-off: stiffening the frame with bracing tends to increase raft rotation under records with stronger short-period content (Northridge, Imperial Valley) because the reduced superstructure deformation channels more seismic demand into the foundation. For Kocaeli, where the building behaves less stiff (with larger drifts and displacements), rotations in braced and unbraced systems become similar, highlighting that rotation response depends on both layout and spectral characteristics of the input. Settlement responses vary by record: in Northridge, braced schemes accumulate more permanent settlement than the unbraced frame, consistent with the increased foundation demands. In Kocaeli, bracing reduces oscillations and permanent settlement compared to the unbraced system. These findings emphasize that improving drift does not automatically improve foundation serviceability under SSI. From a design perspective, these results suggest that bracing layout selection should be SSI-aware rather than relying on fixed-base rankings. K/X layouts are strong choices for drift control, but designers should pair drift checks with explicit verification of raft bearing, rotation, and settlement limits—particularly for motions rich in short-period content, where bracing benefits (and foundation demands) are greatest. For longer-period motions like Kocaeli, expect smaller drift gains and less differentiation in rotation across layouts, with roof-drift benefits secondary to story-wise IDR control. In conclusion, while the configuration hierarchy (K≈X > V≈Inverted-V > Diagonal) remains valid, the magnitude of benefits and the collateral demands on the foundation depend on ground-motion characteristics and SSI. Practical design should balance code-drift targets with foundation serviceability, using site-appropriate motions and SSI-consistent models to avoid unintended penalties for rotation and settlement.

6. Sensitivity / Robustness Checks

To check if the headline findings were influenced by modeling choices or just random parameter selections, a small set of plausible variations was applied to the baseline. First, the mesh and boundaries were refined near the raft, using a coarseness factor of 0.3 near the raft and 1.0 for the far field, confirming that the global trends—K/X being the best for IDR reduction and diagonal being the least effective—remained unchanged. The free-field sides and compliant base were kept the same. The input motions were then re-run using three recorded inputs applied at the compliant base (Northridge at 0.568 g, Imperial Valley at 0.29 g, and Kocaeli at 0.20 g), and the ranking of bracing efficiencies stayed consistent across spectra with different period content. Variations in small-strain stiffness and damping of the soil were also tested, and after adjusting the HSsmall stiffness within reasonable bounds and adding supplemental Rayleigh damping ($\alpha \approx 0.385$, $\beta \approx 0.005$), the SSI-induced period elongation remained visible and the brace-ranking by drift was robust.

The axial rigidity of the braces was checked by modeling them as axial-only with node-to-node anchors using CHS 139.7×4 mm and setting the EA from E=210 GPa. After testing small variations in EA, the relative ordering of the bracing configurations (K/X > V/Inv-V > Diagonal for drift) was unaffected. For the foundation idealization, the raft was kept quasi-rigid (E=30.1 GPa, ν=0.20) with 1 meter of embedment. The mesh around the edges was slightly adjusted, and the qualitative rotation/settlement trade-offs remained the same. Overall, the main conclusions—SSI-induced period elongation and the consistent drift ranking across different bracing types—were found to be stable and unaffected by these reasonable variations.

7. Limitations

This study adopts several simplifying assumptions that bound the interpretation of results:
1-2D plane-strain idealization. The frame–soil system is modeled in 2D (plane strain) to isolate brace/SSI mechanisms; true 3D effects (torsion, plan-irregularities, out-of-plane brace behavior) are not captured.
2-Axial-only bracing. Braces are represented as axial elements (no flexure/shear), appropriate for concentrically braced frames but not capturing brace buckling, yielding, or connection nonlinearity.
3-Linear elastic raft & modest embedment. The raft is quasi-rigid and linearly elastic with ~1 m embedment; nonlinear foundation behavior (gapping/cracking of concrete) is neglected.
4-Soil model scope. HSsmall is used with drained conditions and supplemental Rayleigh damping; groundwater/pore-pressure transients are not activated in dynamics, so liquefaction and cyclic softening are outside scope.
5-Ground-motion set. Only three 20 s records are considered; while deliberately diverse in PGA and spectral content, a broader suite would better quantify record-to-record variability.

These choices keep the model tractable and targeted, but they mean the numerical trends should be read as comparative insights across bracing schemes under SSI—not as design-ready absolutes.

8. Conclusion

SSI elongates the fundamental period and alters demands, with free-vibration checks confirming period lengthening when flexible soil is included, especially for soft to medium clays under raft foundations. Bracing is consistently effective in reducing drift under SSI, but its effectiveness varies: K- and X-bracing deliver the largest reductions (~44–48% for Northridge, ~42–47% for Imperial Valley, and ~31–37% for Kocaeli), followed by V/inverted-V, with single-diagonal being the least effective. Roof displacement improvements are modest, with drift reductions translating to smaller changes in roof-relative displacements (typically a few to ~10%), and occasional slight increases for single-diagonal under certain pulses due to brace force reversals.
Foundation demands can rise with stiffer superstructures, as increased superstructure stiffness can amplify raft rotation and permanent settlement, particularly for stronger, shorter-period inputs like Northridge and Imperial Valley. For longer-period motions like Kocaeli, braced vs. unbraced rotations were more similar, with more moderated settlements. This highlights a drift-versus-foundation trade-off under SSI. When SSI is significant, selecting a bracing scheme based solely on fixed-base rankings may be misleading; K/X bracing layouts are effective for drift control, but their selection should be combined with foundation checks for rotation and settlement, and where necessary, additional foundation stiffening or embedment strategies. Future work should focus on extending to 3D frames, including brace and connection nonlinearities, expanding the motion set, and incorporating pore-pressure generation to strengthen the external validity and refine practice recommendations.

9. References

1-V. Hirave and M. Kalyanshetti, "Seismic response of steel braced building frame considering soil structure interaction (SSI): an experimental study," J. Inst. Eng. India Ser. A, vol. 99, no. 1, pp. 113–122, 2018.
2-G. Basavanagowda, R. Gowda, and M. S. Prashanth Sunagar, "Seismic Response of Steel Braced Vertically Irregular RC Frame Considering Soil Structure Interaction".
3-Université de Jijel, D. Guerdouh, S. Khalfallah, and Ecole Nationale Polytechnique, "Soil-structure interaction effects on the seismic performance of frame structures," Rev. Constr., vol. 18, no. 2, pp. 349–363, 2019, doi: 10.7764/RDLC.18.2.349.
4-M. Kuladeepu, G. Narayana, and B. Narendra, "Soil structure interaction effect on dynamic behavior of 3D building frames with raft footing," Int. J. Res. Eng. Technol., vol. 4, no. 7, pp. 87–91, 2015.
5-M. A. Abdulaziz, M. J. Hamood, and M. Y. Fattah, "A review study on seismic behavior of individual and adjacent structures considering the soil – Structure interaction," Structures, vol. 52, pp. 348–369, June 2023, doi: 10.1016/j.istruc.2023.03.186.
6-M. Kalyanshetti and V. Hirave, "SEISMIC RESPONSE OF COMPOSITE BUILDING FRAME WITH ALTERNATE BRACING SYSTEM CONSIDERING SOIL STRUCTURE INTERACTION (SSI)".
7-M. A. E. Al-Hamdani and G. G. Jumah, "Lateral Seismic Response of Building Frames Under the Influence of Soil–Structure Interaction".
8-L. Di Sarno and A. S. Elnashai, "Bracing systems for seismic retrofitting of steel frames," J. Constr. Steel Res., vol. 65, no. 2, pp. 452–465, Feb. 2009, doi: 10.1016/j.jcsr.2008.02.013.
9-A. Hemmati and A. Kheyroddin, "BEHAVIOR OF LARGE-SCALE BRACING SYSTEM IN TALL BUILDINGS SUBJECTED TO EARTHQUAKE LOADS," J. Civ. Eng. Manag., vol. 19, no. 2, pp. 206–216, Apr. 2013, doi: 10.3846/13923730.2012.741613.
10-V. Anusha and K. R. Reddy, "Retrofitting Of Reinforced Concrete Frames Using Steel Bracings," 2019.
11-M. Rishad and V. Singh, "Modelling of Bracing Systems for Seismic Behaviour of High Rise Steel Building," Des. Constr. Maint., vol. 3, pp. 86–91, 2023.
12-D. D. Ahiwale, D.-P. N. Kontoni, and P. L. Darekar, "Seismic performance assessment of reinforced concrete frames with different bracing systems," Innov. Infrastruct. Solut., vol. 8, no. 3, p. 102, Mar. 2023, doi: 10.1007/s41062-023-01071-3.
13-S. Wichman, J. W. Berman, D. E. Lehman, L. Star, and J. Moresco, "Factors affecting the seismic collapse performance of realistic low-rise braced frame buildings, including soil structure interaction and foundation flexibility," Earthq. Eng. Struct. Dyn., vol. 51, no. 10, pp. 2335–2356, 2022.
14-B. Systems, PLAXIS 2D Reference Manual, 2D ed. Exton, PA, USA: Bentley Systems, 2024.
15-R. Brinkgreve, M. Kappert, and P. Bonnier, "Hysteretic damping in a small-strain stiffness model," Proc Num Mod Geomech NUMOG X Rhodes, pp. 737–742, 2007.
16-L. Qian and H. Zhang, "An improved Non-reflecting Boundary Method for Soil-Structure Interaction Analysis," Comput.-Aided Civ. Infrastruct. Eng., vol. 8, no. 4, pp. 291–297, 1993.
17-S. Vaseghiamiri, M. Mahsuli, M. A. Ghannad, and F. Zareian, "Metamodeling Framework for Multivariate Probabilistic Prediction of Story-Drift Profile of Multistory Buildings," J. Struct. Eng., vol. 150, no. 3, p. 04024009, 2024.

18-K. H. Abdelkareem and N. AL-Mekhlafy, "ROOF LATERAL DISPLACEMENT FOR GRAVITY LOAD DESIGNED RC FRAMES SUBJECTED TO EARTHQUAKES," JES J. Eng. Sci., vol. 42, no. 3, pp. 652–665, May 2014, doi: 10.21608/jesaun.2014.115016.
19-D.-K. Kim, S.-H. Lee, D.-S. Kim, Y. W. Choo, and H.-G. Park, "Rocking effect of a mat foundation on the earthquake response of structures," J. Geotech. Geoenvironmental Eng., vol. 141, no. 1, p. 04014085, 2015.
20-H. Shang, C. Bao, H. Wang, X. Ma, J. Cao, and J. Du, "Seismic response analysis of frame structures with uneven settlement of foundation considering soil-structure interaction," Results Eng., vol. 20, p. 101574, Dec. 2023, doi: 10.1016/j.rineng.2023.101574.
21-P. M. Yesane, Y. Ghugal, and R. Wankhade, "Study on soil-structure interaction: a review," Int J Eng Res, vol. 5, no. 3, pp. 737–741, 2016.
22-K. Edip, M. Garevski, V. Sheshov, and J. Bojadjieva, "Boundary Effects in Simulation of Soil-Structure Interaction Problems," Soil Mech. Found. Eng., vol. 54, no. 4, pp. 239–243, Sept. 2017, doi: 10.1007/s11204-017-9464-2.
23-R. Uliniarz, "Small Strain Soil Constitutive Models HS-SMALL & RU+ MCC–Calibration and Verification," in IOP Conference Series: Materials Science and Engineering, IOP Publishing, 2019, p. 042030.
24-B.-C. B. Hsiung and S.-D. Dao, "Evaluation of constitutive soil models for predicting movements caused by a deep excavation in sands," Electron J Geotech Eng, vol. 19, pp. 17325–17344, 2014.
25-O. C. Zienkiewicz and R. L. Taylor, "The Finite Element Method, Vol. 2: Solid and Fluid Mechanics, Dynamics and Non-linearity," McGraw-Hill Lond. 1991 Pp, vol. 269, 1991.
26-T. J. Hughes, The finite element method: linear static and dynamic finite element analysis. Courier Corporation, 2012.
27-B. Fatahi, B. Huang, N. Yeganeh, S. Terzaghi, and S. Banerjee, "Three-Dimensional Simulation of Seismic Slope–Foundation–Structure Interaction for Buildings Near Shallow Slopes," Int. J. Geomech., vol. 20, no. 1, p. 04019140, Jan. 2020, doi: 10.1061/(ASCE)GM.1943-5622.0001529.
28-T. Benz, Small-strain stiffness of soils and its numerical consequences. in Mitteilung / Institut für Geotechnik Stuttgart, no. 55. Stuttgart: Inst. für Geotechnik, 2007.
29-J. Lysmer, T. Udaka, C. Tsai, and H. B. Seed, "FLUSH-A computer program for approximate 3-D analysis of soil-structure interaction problems," California Univ., Richmond (USA). Earthquake Engineering Research Center, 1975.
30-R. L. Kuhlemeyer and J. Lysmer, "Finite element method accuracy for wave propagation problems," J. Soil Mech. Found. Div., vol. 99, no. 5, pp. 421–427, 1973.
31-W. B. Joyner and A. T. Chen, "Calculation of nonlinear ground response in earthquakes," Bull. Seismol. Soc. Am., vol. 65, no. 5, pp. 1315–1336, 1975.
32-E. Boru and E. Aydin, "The Effect of Different Steel Brace Types on Reinforced Concrete Frame System Retrofit," Türk Doğa Ve Fen Derg., vol. 11, no. 2, pp. 118–124, June 2022, doi: 10.46810/tdfd.1078643.
33-"Standard B (2005) Eurocode 8: Design of structures for earthquake resistance. Part, 1, 1998-1."